Environmental Science & Technology

pubs.acs.org/est

Article

Increases in Global and East Asian Nitrogen Trifluoride (NF_3) Emissions Inferred from Atmospheric Observations

Yu Liu,* Jianxiong Sheng, Matthew Rigby, Anita Ganesan, Jooil Kim, Luke M. Western, Jens Mühle, Sunyoung Park, Hyeri Park, Ray F. Weiss, Peter K. Salameh, Simon O'Doherty, Dickon Young, Paul B. Krummel, Martin K. Vollmer, Stefan Reimann, Chris R. Lunder, and Ronald G. Prinn*

Cite This: *Environ. Sci. Technol.* 2024, 58, 13318−13326

Read Online

ACCESS | Metrics & More | Article Recommendations | Supporting Information

ABSTRACT: Nitrogen trifluoride (NF_3) is a potent and long-lived greenhouse gas that is widely used in the manufacture of semiconductors, photovoltaic cells, and flat panel displays. Using atmospheric observations from eight monitoring stations from the Advanced Global Atmospheric Gases Experiment (AGAGE) and inverse modeling with a global 3-D atmospheric chemical transport model (GEOS-Chem), we quantify global and regional NF_3 emission from 2015 to 2021. We find that global emissions have grown from 1.93 ± 0.58 Gg yr^{-1} (± one standard deviation) in 2015 to 3.38 ± 0.61 Gg yr^{-1} in 2021, with an average annual increase of 10% yr^{-1}. The available observations allow us to attribute significant emissions to China (0.93 ± 0.15 Gg yr^{-1} in 2015 and 1.53 ± 0.20 Gg yr^{-1} in 2021) and South Korea (0.38 ± 0.07 Gg yr^{-1} to 0.65 ± 0.10 Gg yr^{-1}). East Asia contributes around 73% of the global NF_3 emission increase from 2015 to 2021: approximately 41% of the increase is from emissions from China (with Taiwan included), 19% from South Korea, and 13% from Japan. For Japan, which is the only one of these three countries to submit annual NF_3 emissions to UNFCCC, our bottom-up and top-down estimates are higher than reported. With increasing demand for electronics, especially flat panel displays, emissions are expected to further increase in the future.

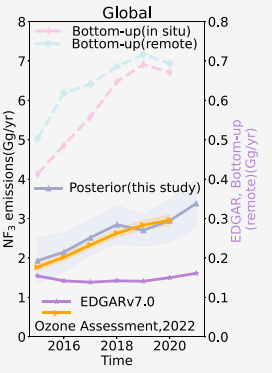

KEYWORDS: *nitrogen trifluoride, GEOS-Chem, AGAGE, top-down, global and regional NF_3 emission*

INTRODUCTION

Nitrogen trifluoride (NF_3) is a very potent long-lived greenhouse gas (GHG), with an atmospheric lifetime of approximately 569 years[1] (uncertainty in the lifetime is thought to be large[2,3]), and an extremely high global warming potential (17,200 on a 100-year time scale).[4,5] It is primarily emitted during NF_3 production and from its end use in the cleaning of silicon-containing deposits in the semiconductor industry or during the manufacture of flat-panel displays (FPD), such as liquid crystal displays (LCDs) and amorphous-Si/crystalline-Si thin-film photovoltaic (PV) cells.[6−9] Minor emissions are thought to be associated with its use as a rocket fuel oxidizer, as a fluorine donor for chemical lasers, and for fluorochemical production.[6,10] Leakage during its transportation likely has a negligible contribution to the atmospheric NF_3 abundance.[8] The removal of NF_3 in the atmosphere is mainly through photolysis in the stratosphere and mesosphere.[11,12]

NF_3 was included in the basket of substances controlled under the Kyoto Protocol through the Doha Amendment in 2012. Some countries have specific targets to reduce NF_3 emissions as part of their wider greenhouse gas emissions reduction strategy, e.g., Japan aimed for reduction from 1.6 million tons CO_2-eq in 2013 to 0.5 million tons CO_2-eq in 2030.[13] NF_3 emissions have also been required to be reported to the Chinese government since 2021.[14] South Korea, one of the major emitters,[7] does not report its NF_3 emissions to the United Nations Framework Convention on Climate Change (UNFCCC) or include it in their commitments to the Paris agreement.[15] Other Annex I Parties (such as USA, Canada, and countries in the European Union and Oceania) have a bulk reduction commitment to UNFCCC, but do not single out NF_3 emissions reduction.[16−20]

Previous studies showed that global NF_3 emissions had risen from undetectable levels in the 1980s to 1.18 ± 0.21 Gg·yr^{-1} in 2011, based on inverse modeling using a 12-box atmospheric chemistry transport model combined with atmospheric measurements.[6] The latest World Meteorological Organization Scientific Assessment of Ozone Depletion reported that NF_3 emissions increased from 2.0 ± 0.1 Gg·yr^{-1} in 2016 to 3.0 ± 0.1 Gg yr^{-1} in 2020, based on results from the 12-box model and measurements at five AGAGE stations.[5]

Emissions from East Asia were estimated for 2014 and 2015 by Arnold et al.[7] In that study, emissions from South Korea

Received: May 6, 2024
Revised: June 27, 2024
Accepted: June 28, 2024
Published: July 15, 2024

were estimated to be approximately 0.4 ± 0.05 and 0.6 ± 0.07 Gg yr^{-1} in 2014 and 2015, respectively. Emissions from China were found to be potentially substantial but were inferred with very large uncertainties (1.08 ± 1.17 and 0.36 ± 1.36 Gg yr^{-1} in 2014 and 2015, respectively).

In this study, we estimate global and regional emissions from 2015 to 2021, using a global inversion system based on a 3-D chemical transport model, GEOS-Chem, and observational data from eight AGAGE stations: Kennaook/Cape Grim, Tasmania, Australia (CGO), Cape Matatula, American Samoa (SMO), Ragged Point, Barbados (RPB), Gosan, South Korea (GSN), Trinidad Head, California, USA (THD), Jungfraujoch, Switzerland (JFJ), Mace Head, Ireland (MHD), and Zeppelin, Svalbard, Norway (ZEP) (Supplementary Table 1).[21] A major advance of this study is that the inversion system uses a high resolution (2.5° longitude and 2° latitude) global 3-D chemical transport model, will account for interannual variability in the meteorological fields, and also resolves continental scale emissions rather than zonal averages, compared to previously used box models.

GROWTH IN GLOBAL MOLE FRACTIONS

A previous study reported that the global tropospheric annual mean dry air mole fraction increased from almost zero in the early 1970s (0.008 ppt in 1975) to 0.86 ± 0.04 parts per trillion (ppt) in 2011, based on archived air data samples.[6] Updated reported values, including in situ measurements, show that this growth continued, reaching to 2.3 ppt in 2020.[5] Data updated here from observations at AGAGE measurement sites show that NF_3 global mean mole fractions reached 2.59 ± 0.11 ppt in 2021 (Figure 1). The mean growth rate of the global mole fraction between 2015 and 2021 was 0.22 ± 0.12 ppt yr^{-1}. This value reached a maximum in 2021 (0.28 ± 0.15 ppt yr^{-1}), suggesting that global emissions have continued to grow throughout this period.

Increases in Global Emissions. Here, we report inferred emissions from three inversions using three different a priori spatial distributions. The prior annual mean emissions are extrapolated from Arnold et al.[6] The three prior distributions are derived from proportions of semiconductor (wafer) capacity, flat screen display capacity (as most of the flat screen display production is for liquid-crystal displays (LCDs), we assume that all flat screen production is for LCD throughout), or NF_3 market share for each region (we assume NF_3 market share represents the NF_3 consumption from each region in Supplementary Table 2 and regions are defined in Supplementary Figure 1). Global posterior emissions are the total of the derived NF_3 emissions from 11 regions defined in Supplementary Figure 1. The amount of NF_3 employed in the photovoltaic (PV) cell industry only accounts for a small fraction of global NF_3 production (about 3%[8]), so we do not include this sector in our prior emission distribution estimates.

The mean inversion results show that global emissions of NF_3 rose from 1.93 ± 0.58 Gg yr^{-1} in 2015 to 3.38 ± 0.61 Gg yr^{-1} in 2021, with an average annual increase of 10% yr^{-1}, with large error reduction (>80%) compared to the prior uncertainty (Figure 2 and Supplementary Figures 2–5). Note that the average of the inversion results using the three different prior estimates is presented, unless otherwise stated. The overall emission growth rate derived using a linear regression for the time period 2015–2021 was significantly positive, at 0.70 ± 0.06 Gg yr^{-2}.

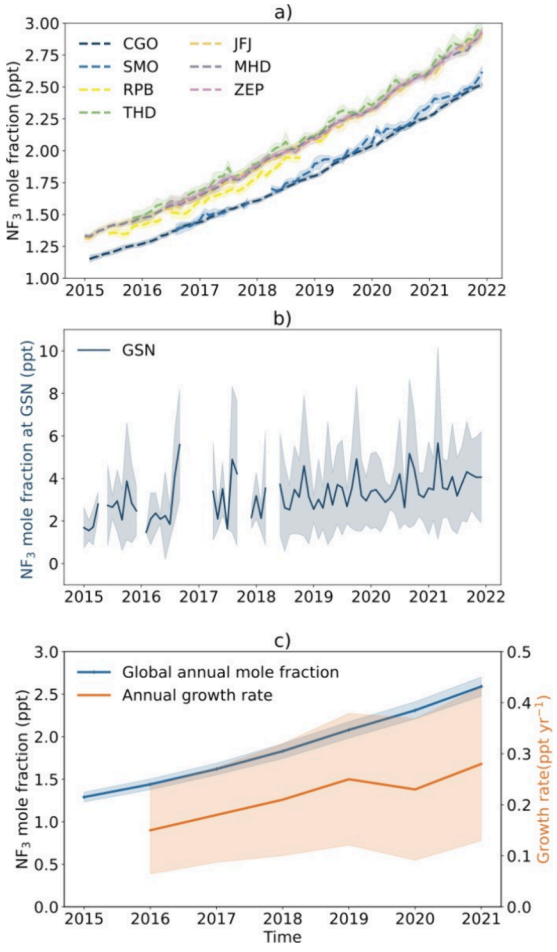

Figure 1. Monthly mean NF_3 mole fractions and their standard deviations in monthly variability measured at (a) seven AGAGE stations in relatively remote locations: CGO: Cape Grim, Tasmania; SMO: Cape Matatula, American Samoa; RPB: Ragged Point, Barbados; THD: Trinidad Head, California; JFJ: Jungfraujoch, Switzerland; MHD: Mace Head, Ireland; ZEP: Zeppelin, Norway; (b) monthly mean NF_3 mole fractions and their standard deviations in monthly variability measured at GSN: Gosan, South Korea; (c) global annual mole fraction and annual growth rate. Global annual mole fractions are from the average of the monthly mean NF_3 mole fractions from five background sites (CGO, SMO, RPB, THD, MHD).

The model simulations agree well with the observed trend, as shown by the comparison of the posterior mole fraction and the observations (Supplementary Figures 6–7). Supplementary Table 3 shows that the three inversion simulations improve the model and observation root-mean-square error compared to the prior.

Emissions from East Asian Regions. Emissions were estimated from 11 regions (Supplementary Table 4). Among these regions, East Asia emits large amounts of NF_3 to the global totals (>70%). Since East Asia is the main contributor to global emissions and their variability, this section focuses on that region.

We separately quantify East Asian emissions from south China, northeast China, South Korea, and Japan. Emissions from the rest of China and North Korea are negligible, and these two regions are included into the region defined as the rest of Asia, Russia, and middle east (Figure 2, Supplementary Figures 2–3). The inferred mean annual emissions from south

https://doi.org/10.1021/acs.est.4c04507
Environ. Sci. Technol. 2024, 58, 13318−13326

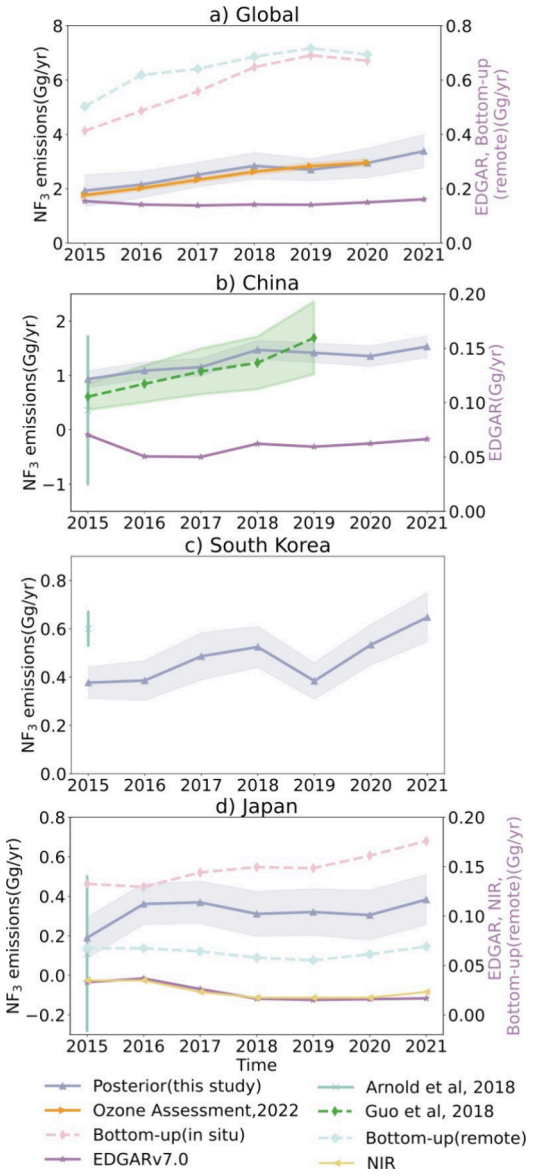

Figure 2. Comparisons of top-down from this study to bottom-up estimates and previous studies: (a) Global compared to EDGAR v7.0[26] and Laube & Tegtmeier[5]; (b) China (with Taiwan included) compared to EDGAR v7.0, Guo et al.[27] and Arnold et al.[7]; (c) South Korea compared to Arnold et al.[7]; (d) Japan compared to data from EDGAR v7.0, Japan's 2023 National Inventory Report to the UNFCCC (NIR, Japan),[10] Arnold et al.[7] For (a) Global and (d) Japan, we also show bottom-up (in situ) (in situ meaning low NF_3 conversion rate) and bottom-up (remote) (remote meaning high NF_3 conversion rate) emissions estimated in this study with no abatement (destruction of NF_3 in exhaust gas) considered, while NIR (Japan, 2023) data state that abatement was considered. Top-down results and bottom-up (in situ) are sharing the left *y*-axis, while EDGAR v7.0, NIR, bottom-up (remote) are using the right *y*-axis. Note that the left *y*-axis is 10 times higher than the right *y*-axis and bottom-up (in situ) results are around 10 time larger than results from bottom-up (remote).

China and northeast China are 0.83 ± 0.13 and 0.45 ± 0.12 Gg yr^{-1} between 2015 and 2021, respectively. The contribution of the mean annual emissions from these two regions to the global emissions (2.64 ± 0.51 Gg yr^{-1}) varies between 22% and 45% for south China and 11% and 27% for northeast China over this seven-year period. South Korea has an average emission of 0.48 ± 0.08 Gg yr^{-1} between 2015 and 2021, and its emissions comprise 12−26% of the inferred average global mean emissions over the seven years. Given the proportion of semiconductors and flat panel display-LCDs manufactured in South Korea relative to global totals (24% for LCD capacity in 2018, 26% for semiconductor capacity in 2015),[22,23] we conclude that this ratio is reasonably consistent with the industrial activities in South Korea. The emissions from Japan are lowest in this region, with average emissions of 0.32 ± 0.10 Gg yr^{-1}, contributing 7−20% of global emissions.

NF_3 emissions have increased between 2015 and 2021 by 0.34 ± 0.18 Gg yr^{-1} and 0.26 ± 0.17 Gg yr^{-1} in south China and northeast China, respectively, while global emissions have risen by 1.45 ± 0.84 Gg yr^{-1} (see Supplementary Table 5). Hence, NF_3 emissions growth from China contributed around 41% of the global rise. Emissions growth in South Korea (0.27 ± 0.12 Gg yr^{-1}) and Japan (0.19 ± 0.16 Gg yr^{-1}) over this period contributed 19% and 13% to the rise, respectively. The increases from these three countries together have contributed approximately 73% of the global increase (Supplementary Table 5).

The influence of COVID-19 on the estimated NF_3 emissions seems small in South Korea; even during the 2020−2021 period in which there were national lockdowns, and NF_3 related activities, such as factory production, trading, were less active, the emissions still increased. The derived NF_3 emissions between 2020 and 2021 increased by 0.15 ± 0.12 Gg yr^{-1} compared to the period of 2015 to 2018 (2019 is not considered here as there were trade conflicts between Japan and South Korea in 2019,[24] when the limited raw material supply to produce semiconductors might affect the NF_3 consumption related activities in South Korea). In contrast, we do not find a significant rise in emissions from South China, Northeast China, and Japan during the COVID-19 period (2020−2021) compared to the period before (2015−2019) (0.12 ± 0.19 Gg yr^{-1} for South China, 0.07 ± 0.17 Gg yr^{-1} for Northeast China, 0.03 ± 0.16 Gg yr^{-1} for Japan).

Emissions from Other Regions. Regions outside of East Asia contributed around 21% to the global averaged NF_3 emissions and 27% to the global emission increase (Supplementary Figures 2−3).

Among the rest of the regions, only three regions have significant emission growth between 2015 and 2021: 13% (0.19 ± 0.16 Gg yr^{-1}) from North America, 12% (0.18 ± 0.09 Gg yr^{-1}) from Europe, and 4% (0.06 ± 0.4 Gg yr^{-1}) from Oceania. Only North America released above zero emissions averaged over 7 years (2015−2021) (0.29 ± 0.10 Gg yr^{-1}). The estimated averaged emissions in Europe and Oceania are not significantly different from zero.

Southeast Asia emitted 0.18 ± 0.13 Gg yr^{-1} on average, with no significant increase in the estimation in 2021 compared to 2015. The estimated annual mean emissions decreased in between 2020 and 2021 compared to 2018 and 2019, which might reflect the influence of lockdown on the NF_3 related industrial activity in this region during the COVID-19 period.

The remaining regions (South Asia, Africa, Central and South America) neither have large emissions, nor significant emissions growth. The emissions from South Asia (defined as India, Sri Lanka, Pakistan and Bangladesh) have changed from 0.15 ± 0.10 Gg yr^{-1} in 2015 to 0.08 ± 0.13 Gg yr^{-1} in 2021, with emissions reduced by around 5%, which is offset by the increase in Southeast Asia. The mean emission for Africa is 0.02 ± 0.11 Gg yr^{-1} over 2015 and 2021, and the average

https://doi.org/10.1021/acs.est.4c04507
Environ. Sci. Technol. 2024, 58, 13318−13326

emissions in Central and South America is not significantly from zero. This is consistent with the low NF_3-related industrial activities in these two regions over this time period (see Supplementary Table 2 and 4). Supplementary Figure 6 shows the error reduction in each region. Even though there are no AGAGE continuous observation network in these regions (South Asia, Africa, Central and South America, Southeast Asia), the errors are still reduced based on constraint from other observations.

DISCUSSION

Comparison to Previous Top-Down and Bottom-Up Results. Global emissions derived over the period 2015−2020 using five AGAGE stations and the AGAGE 12-box model are consistent, within 1-sigma uncertainties, with our global estimates (Figure 2).[5] The two top-down methods suggest that emissions of NF_3 are more than 10 times higher than the EDGAR v7.0 estimate during this period (Figure 2) (EDGAR, 2022). Moreover, top-down emissions have continuously increased since 2015, unlike those from EDGAR v7.0. The discrepancy between top-down and EDGAR v7.0 estimates might be due to underestimation of emissions factors by EDGAR v7.0 or emissions from certain source sectors or countries might be missing. For example, EDGAR v7.0 does not include any NF_3 emissions in South Korea, even though this country plays an important role in the semiconductor and LCD industries; EDGAR v7.0 only considers NF_3 emissions from the electronic sectors, while other processes, such as the process of producing NF_3, and other industry activities that use NF_3 (e.g., NF_3 usage in lasers), which may significantly contribute to the NF_3 emissions, are not included in EDGAR v7.0.[6,10,30]

The derived NF_3 emission for China (with Taiwan included) in this study in 2015 is statistically consistent with that was estimated in a previous study (0.98 ± 0.15 $Gg{\cdot}yr^{-1}$ compared to 0.36 ± 1.38 $Gg{\cdot}yr^{-1}$, as shown in Figure 2 and Arnold et al.[7]), although the previous study is very uncertain. Our mean posterior estimate for China is more than twice that from Arnold et al.[7] Our estimate for South Korea (0.35 ± 0.07 $Gg{\cdot}yr^{-1}$) is significantly smaller than that of Arnold et al.[7] in 2015 (0.6 ± 0.07 $Gg{\cdot}yr^{-1}$), while the estimate for Japan (0.20 ± 0.1 $Gg{\cdot}yr^{-1}$) is comparable to their top-down result (0.11 ± 0.39 $Gg{\cdot}yr^{-1}$). Similar to our significantly higher global NF_3 top-down emissions compared to EDGAR v7.0, the regional top-down estimated emissions for China and Japan are an order of magnitude higher than the emissions estimated by EDGAR v7.0 (Figure 2). The annual mean estimates in this top-down study suggest that emissions from Japan declined during 2017−2018, consistent with the trend estimated by EDGAR v7.0 and the National Inventory Report to the UNFCCC (NIR, Japan), although higher absolute emissions for Japan are derived in this study (NIR estimate of emission reductions between this time frame were mainly driven by the reduction in production emissions, shown in the method section Bottom-Up Estimates for Japan).[10,26]

Robustness of Inversion Results. Sensitivity tests were performed to assess whether inversion results are sensitive to the network configuration, prior emissions magnitude, trend and uncertainty, and observational error (Supplementary Figures 8−13). The only significant difference from our main results is in the emissions from South Korea when observations from GSN station are not included. As there are some data gaps at this station in 2016, 2017, and 2018 due to instrumental damage by typhoons,[25] we do not know whether the variability in NF_3 emission from South Korea is caused by the data gaps or by actual changes in emissions.

It is also possible that emissions from small countries such as South Korea may be impacted by model resolution. It is difficult to assess the impact of model resolution alone, but the sensitivity of South Korean emissions to the inclusion or exclusion of Gosan, and the difference of our results with Arnold et al. (2018) may in part be related to the relatively course resolution of the model compared to the size of that country and its proximity to the Gosan.

Relating Emissions to Industrial Activity. Our global estimated posterior NF_3 emissions account for less than 10% of the global NF_3 production (Figure 3 upper panel, Supplementary Table 6), and this emission ratio, defined as posterior global NF_3 emissions divided by global production, was used to explain the change of the efficiency of industrial processes.[6] The emission ratio has significantly declined between 2017 (0.09 ± 0.02) and 2020 (0.07 ± 0.01). The emission ratio in 2019 is also significantly smaller than the ratio for 2011, as calculated by Arnold et al.[6] This sustained reduction of the emission ratios could point to lower NF_3 production related emissions, higher NF_3 use efficiencies and/or more widespread of remote plasma sources (RPS) or more efficient abatement measures in the waste streams of facilities that use NF_3.[31−33]

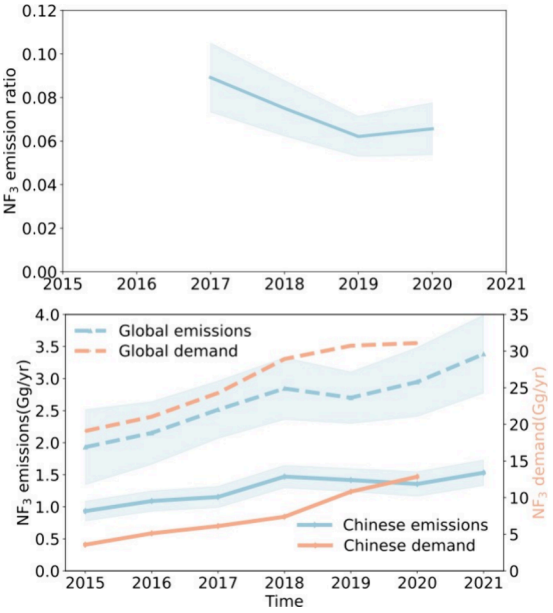

Figure 3. Upper panel: emission ratio (unitless) of posterior global NF_3 emissions to global production. Global production is the total annual amount of NF_3 produced globally. Lower panel: comparison of global and Chinese NF_3 emissions and demand. Demand is the total amount of NF_3 needed or required by the industrial companies globally or in China. The global NF_3 production data, global demand data between 2017 and 2020 and Chinese demand (not including Taiwan) are from m.huaon.com,[28] and the global demand data in 2015 and 2016 are from Adams.[29]

The estimated global posterior emissions follow a similar trend to global NF_3-related industrial activities, i.e., NF_3 demand data (Figure 3 lower panel). The significant increase in Chinese emissions until 2018 is consistent with increasing Chinese NF_3 demand data (Figure 3 lower panel, Supplementary Table 7). Our estimated Chinese emissions do not

https://doi.org/10.1021/acs.est.4c04507
Environ. Sci. Technol. 2024, 58, 13318−13326

increase as fast as Chinese NF_3 demand after 2018, which might point to lower NF_3 production-related emissions, higher NF_3 utilization efficiency, or more widespread or more efficient abatement.

We derived two bottom-up emission estimates for Japan based on the NF_3 production and consumption data in the Japanese NIR. In both estimates, we consider zero abatement to assess the upper limit of emissions but apply different usage rates based on two NF_3 consumption methods: (a) in situ, in which the NF_3 cleaning process is analogous to the process for other cleaning gases like C_2F_6 and C_3F_8, characterized by low NF_3 use efficiency and high NF_3 emissions without abatement); (b) remote, in which remote plasma clean is used, characterized by high NF_3 use efficiency and low NF_3 emissions without abatement. If we assume that 100% of the NF_3 is consumed by the semiconductor and LCD production in the in situ method, our estimated upper limit emissions would have increased from 0.463 to 0.680 Gg·yr^{-1} from 2015 to 2021 (Figure 2 d). In most years, these values would be higher than the top-down emissions. If we assume that 100% of the NF_3 is used in the remote method, our estimated emissions would have only increased from 0.067 to 0.069 Gg·yr^{-1}, which would be about 80% lower than our top-down emissions estimate, but still higher than the NF_3 emissions reported in the Japanese NIR. The Japanese NIR does not report the proportion in which the two methods are used, but since our top-down emission estimate is significantly higher than the Japanese NIR emissions estimate, we suggest that some of the assumptions in the Japanese NIR, such as abatement rates, and/or the data used in the NIR, such as estimated emissions from production and industrial activities, need to be revised. Estimated emissions using the in situ and remote method from Japan account for around 10% and 9% of our bottom-up estimated global emissions using similar parameters (details shown in the Bottom-up Estimates section in Methods), respectively, which are consistent with our top-down estimated ratio (7−20%, as shown above). Our results suggest that real-world abatement efficiencies may be lower than that used for estimating Japanese NIR emissions, in line with the conclusions derived for CF_4 and C_2F_6 by Kim et al.,[34] even though NF_3 is much easier to abate than CF_4 or C_2F_6.

Our derived global emissions increased from 1.93 ± 0.58 Gg yr^{-1} (±one standard deviation) in 2015 to 3.38 ± 0.61 Gg yr^{-1} in 2021, significantly larger than that from a bottom-up inventory (EDGAR v7.0). The derived emissions are also significantly higher than EDGAR v7.0 estimates in China and Japan. East Asia contributes to around 73% of the global NF_3 emission increase from 2015 to 2021, and North America, Oceania, and Europe contributed most of the remaining growth. We could only estimate the bottom-up emissions for Japan and evaluate Japanese NIR emissions in this study, as most countries do not report their NF_3 consumption and production data. We find that the uncertainties for the bottom-up estimates are difficult to calculate due to the incompleteness of the data. It would be very helpful if details such as NF_3 consumption and production data, usage rates, abatement rates, etc. were included in future NIRs. When combined with top-down emission estimates such as those presented here, this data would provide new insights to improve bottom-up methods and resulting emission inventories.

METHODS

Measurement Data. The Medusa AGAGE gas chromatograph with mass spectrometric detection (GC-MS "Medusa") was the first instrument used to regularly monitor in situ NF_3 dry mole fractions worldwide.[21,35] Continuous atmospheric NF_3 measurements were implemented at AGAGE sites since 2011, with ambient measurements roughly every 2 h and precisions that improved from ∼2% to ∼1% (or better) due to improvements in analytical methods, chromatographic peak sizes, and mass spectrometer technology.[21,35] NF_3 measurements are reported on the Scripps Institution of Oceanography (SIO) SIO-12 primary calibration scale.[21] Every ambient air measurement is followed by a working standard measurement to account for changes in detector response. Each working standard is compared with a tertiary standard four times a week. Calibrated tertiary standards are sent by SIO to each measurement site and they are reanalyzed at SIO upon their return. Information for the measurement sites used for the inversion is listed in Supplementary Table 1. Mole fractions at the eight AGAGE stations are used to estimate global and regional emissions, while unpolluted filtered data are used to generate the global initial conditions. The unpolluted filtered data for a particular day are identified as the data within median plus 2σ, after removing seasonal variation using a moving window with 121 days periods (60 days before and 60 days after the current day).[36] Global annual mean mole fractions are calculated based on global monthly nonpolluted mean mole fractions and were taken from the AGAGE Web site https://agage.mit.edu/.

Atmospheric Transport Modeling Using GEOS-Chem. GEOS-Chem is a 3-D global atmospheric chemistry transport model, and we use version 12.5 in this study to conduct the forward simulation and generate the sensitivity matrix used in the inversion.[37] The forcing meteorological data are from Modern-Era Retrospective Analysis for Research and Applications, Version 2 (MERRA2) generated by the NASA Global Modeling and Assimilation Office (GMAO),[38] which drives the model with a resolution of 2.5° longitude and 2° latitude and 45 vertical levels (Supplementary Figure 1). To initialize our simulation, we spun up the model for 5 years prior to the study period, using the prior emissions extrapolated from Arnold et al.[6] At the end of the spin-up period, the simulated mole fraction field was adjusted so that the average mole fraction at the measurement station locations was consistent with the observations. Emissions derived in the first year (2014) of the inversion were discarded to account for any residual impacts of model spin-up.

Offline fields that describe the stratospheric loss of NF_3 were not readily available for use in this study. However, given its very long lifetime compared to the study period, it is unlikely that errors in the stratospheric loss distribution will have a substantial impact on our results. Therefore, for convenience, we decided to simply rescale the stratospheric loss for some readily available species (CH_4 in this case), to provide a reasonable lifetime for NF_3. We iteratively adjusted the loss field until a lifetime of around 531−593 years was achieved (see Supplementary Figure 15). Tests using a substantially larger (around 800−1000 years) lifetime does not result in significant changes in derived emissions (differences less than 0.1% in the global total).

A Priori Emissions and State Vectors. The a priori global annual emissions from 2014 to 2022 are extrapolated

https://doi.org/10.1021/acs.est.4c04507
Environ. Sci. Technol. 2024, 58, 13318−13326

using the regressed trend from the results for 2007−2011 from Arnold et al.[6] The total NF_3 emissions in each year are assigned to 11 different regions based on the prior distribution information from three different resources to generate three inversions: proportions for wafer capacity, flat screen display (LCDs) capacity and NF_3 market share. Information on the NF_3 proportions in each region is summarized in Supplementary Table 2. Here, the information for NF_3 market distribution in 2018 is taken from m.huaon.com[39]; the distribution of LCD production capacity in 2018 from statista.com[22]; the information on wafter capacity for semiconductor in 2015 is taken from Platzer et al.[23]; the regional emissions are redistributed to each grid cell based on the intensity of night light data in 2016 from NASA (https://eoimages.gsfc.nasa.gov/images/imagerecords/144000/144897/BlackMarble_2016_01deg_gray_geo.tif). Night lights data represent both population and industrialization density and were used for approximating the prior distribution of trace gases released from industrial activities in a former study.[40] The final proportions for each region used in this study are listed in the middle column in Supplementary Table 2. We assume constant emissions in each grid throughout the year.

The 11 regions in the state vector are North America; Europe; Africa; central and south America; Oceania; South Asia (India, Sri Lanka, Pakistan and Bangladesh); south China (with Taiwan included); South Korea; Japan; southeast Asia; northeast China (Supplementary Figure 1). East Asia is separated into South China, Northeast China, South Korea, and Japan, as the sensitivity of mole fraction to the emissions changes in the regions from east Asia at the AGAGE measurement sites is different (Supplementary Figure 15). The rest of the world is not optimized and hence not included in the state vector, as the NF_3 related industrial activity is very low, and the NF_3 emissions are negligible according to current available information (e.g., the maximum NF_3 emission is 0.48 $\times 10^{-3}$ Gg yr^{-1} in 2016 in Russia according to UNFCCC data set,[41] which is negligible comparing to the minimum in other region, such as Japan). We estimate emissions for south China (with Taiwan included), northeast China, Japan, and South Korea separately to account for the NF_3 emissions produced by flat screen and semiconductor factories in these regions. In South Asia, only India, Sri Lanka, Pakistan, and Bangladesh are considered in this region, and the remaining countries are assigned to the rest of the world due to the expectation that there are negligible NF_3 emissions from these regions. Turkey is included in the European domain. China is separated into South China (including Hong Kong and Macao plus Taiwan) and Northeast China.

Inversion Theoretical Framework. We optimize the global NF_3 emissions based on Bayes' theorem. The Bayesian cost function J of the inverse problem is written as

$$J(x) = (x - x_A)S_A^{-1}(x - x_A) + (y - Kx)S_O^{-1}(y - Kx)$$

in which x is the state vector. x_A is the prior emissions from different regions. Here, both x and x_A are emissions from 11 regions and 108 months (from 2014 January to 2022 December), leading to 1188 unknowns (Supplementary Figure 1). K is the Jacobian matrix of the monthly sensitivity of modeled NF_3 mole fractions at the measurement sites to the perturbation (10%) of prior NF_3 emissions from the different regions. Here, we track the perturbed emissions for one year and then approximate the remaining sensitivity as a two-year exponentially decay toward the globally well mixed mole fraction,[42] after which, the perturbed emissions are assumed to be well mixed globally. y is the monthly mean difference between the measurements and the mole fractions derived from the simulation with unperturbed prior emissions and thus, x_A is zero, and the posterior emissions represent the deviations from the prior emissions. S_A is the prior state vector covariance, while S_O is the observational and model error covariance. We use 25% of the global annual prior mean emissions as the annual errors (standard deviation) for each region to construct the prior error covariance matrix. 25% is chosen because it is the maximum difference of the proportion information between the semiconductor and LCD in Supplementary Table 2. We assume no spatial correlation between the emissions from different regions and no temporal correlations between different months, so only diagonal elements in the prior error covariance matrix. The observational error covariance matrix S_O is approximated as the standard deviations of monthly mean measurements at each site. Errors of all measurements are assumed to be independent.

By minimizing J, with respect to x, we get the analytical solution for posterior emissions changes:

$$\hat{x} = x_A + G(y - Kx)$$

where G is the gain matrix:

$$G = (K^T S_o^{-1} K + S_A^{-1})^{-1} K^T S_o^{-1}$$

Bottom-Up Estimates. The total bottom-up emissions E (Gg yr^{-1}) is calculated using the following equation:

$$E_{total} = E_{production} + E_{end-use}$$

$E_{production}$ is the NF_3 emitted during NF_3 production, and $E_{end-use}$ is the aggregated NF_3 released during the end use of NF_3 from different industrial activities, mainly semiconductor, LCD, and PV cells. They are calculated using the following equations:

$$E_{production} = P_p \times r_p$$

P_p is the amount of production, and $r_p = E_{production}/P_p$ is the production ratio from all the processes relating to of NF_3 production.

$$E_{end-use} = \sum_{i=1}^{N} (P \times r_{supply}) \times (1 - r_{use})$$

For Japanese bottom-up emissions (Japan being the only country for which the required data is publicly available), N = 2, as there are mainly semiconductor and flat panel display (LCD) industries in this country. P is the total consumed NF_3 amount from all industry activities (tons); r_{supply} is the process supply rate (also known as "heel factor"), 90% is deployed here, meaning 10% of the NF_3 in the cylinders will not be used[43]; r_{use} is the use rate, containing two catalogs: in situ and remote. In-situ NF_3 cleaning process is analogous to the process for other cleaning gases like C_2F_6 and C_3F_8. Remote plasma sources dissociate NF_3 into fluorine radicals before they enter the chamber. For semiconductors, r_{use} is 80% for in situ, 98% for remote; for LCDs, r_{use} is 70% for in situ, 97% for remote.[43] Since the use rate is much lower for NF_3 in situ use, emissions are typically much higher as more unused NF_3 exists in the tools used in manufacturing processes. This can be mitigated by abatement, that is destruction of NF_3 in the waste gas stream. We do not consider abatement for $E_{end-use}$ here.

https://doi.org/10.1021/acs.est.4c04507
Environ. Sci. Technol. 2024, 58, 13318−13326

For global bottom-up emissions, $N = 3$, as production of certain PV cells can also results in NF_3 emissions. We assume that the parameters (r_{use}, r_p) used for Japan also applies to the global scale. The global NF_3 production data and global demand data between 2017 and 2020 are from m.huaon.-com,[28] and the global demand data in 2015 and 2016 are from Adams.[29] The global production in 2015 and 2016 are inferred from our top-down emissions divided by the scaled emission ratio from our study and the value in 2011 from Arnold et al.[6] Here, the proportion of NF_3 consumption used for PV cells among global demand is using 3%, with a total leaking ratio 0.017.[8] The global NF_3 consumption in semiconductor was taken from World Semiconductor Council,[44] while the amount used in LCD is the remaining in the global demand. The calculated total bottom-up emissions for in situ and remote are listed in Supplementary Table 8 and the details of the data are in the supporting Excel files.

■ ASSOCIATED CONTENT

Data Availability Statement

The observation data from AGAGE are available on https://agage.mit.edu/

Supporting Information

The Supporting Information is available free of charge at https://pubs.acs.org/doi/10.1021/acs.est.4c04507.

Table S1: Information about measurement stations from AGAGE; Table S2: Regional percentages of factors used for prior NF_3 emissions; Table S3: Performance of the inversion simulations using RMSE; Table S4: Global and regional annual posterior emissions averaged from three inversion runs; Table S5: Global and regional average emissions over the simulation period; Table S6: Global production, NF_3 emission ratio, and their uncertainties; Table S7: Global demand and Chinese (mainland) demand data; Table S8: Bottom-up estimated emissions for Japan and other regions; Figure S1: Regions used in the inversion; Figure S2: Annual global and regional posterior NF_3 emissions from three inversion runs; Figure S3: Annual global and regional prior and posterior NF_3 emissions from the average of the three inversion runs; Figure S4: Error reduction from the average of the three inversion simulations; Figure S5: Correlations between optimized emissions from the eleven regions; Figure S6: Observed and modeled monthly mean NF_3 mole fractions using the prior and posterior estimates at eight AGAGE measurement sites; Figure S7: Differences between observations and GEOS-Chem modeled monthly mean NF_3mole fractions using the prior and posterior estimates; Figure S8: Sensitivity to different network choices; Figure S9: Sensitivity to different prior emission error; Figure S10: Sensitivity to observational error; Figure S11: Sensitivity to prior emissions magnitude; Figure S12: Sensitivity to prior emissions trend; Figure S13: Sensitivity to constant prior emissions (PDF)

Sectoral bottom-up emissions for global and Japan (XLSX)

■ AUTHOR INFORMATION

Corresponding Authors

Yu Liu − *Center for Global Change Science, Massachusetts Institute of Technology, Cambridge, Massachusetts 02139, United States;* orcid.org/0000-0002-6214-9674; Email: yuliu223@mit.edu

Ronald G. Prinn − *Center for Global Change Science, Massachusetts Institute of Technology, Cambridge, Massachusetts 02139, United States*; Email: rprinn@mit.edu

Authors

Jianxiong Sheng − *Center for Global Change Science, Massachusetts Institute of Technology, Cambridge, Massachusetts 02139, United States;* orcid.org/0000-0002-8008-3883

Matthew Rigby − *Center for Global Change Science, Massachusetts Institute of Technology, Cambridge, Massachusetts 02139, United States; School of Chemistry, University of Bristol, Bristol BS8 1SA, United Kingdom*

Anita Ganesan − *Center for Global Change Science, Massachusetts Institute of Technology, Cambridge, Massachusetts 02139, United States; School of Geographical Sciences, University of Bristol, Bristol BS8 1SS, United Kingdom*

Jooil Kim − *Scripps Institution of Oceanography, University of California San Diego, La Jolla, California 92093, United States*

Luke M. Western − *School of Chemistry, University of Bristol, Bristol BS8 1SA, United Kingdom;* orcid.org/0000-0002-0043-711X

Jens Mühle − *Scripps Institution of Oceanography, University of California San Diego, La Jolla, California 92093, United States;* orcid.org/0000-0001-9776-3642

Sunyoung Park − *Department of Oceanography, Kyungpook National University, Daegu 41566, Republic of Korea*

Hyeri Park − *Department of Oceanography, Kyungpook National University, Daegu 41566, Republic of Korea*

Ray F. Weiss − *Scripps Institution of Oceanography, University of California San Diego, La Jolla, California 92093, United States;* orcid.org/0000-0001-9551-7739

Peter K. Salameh − *Scripps Institution of Oceanography, University of California San Diego, La Jolla, California 92093, United States*

Simon O'Doherty − *School of Chemistry, University of Bristol, Bristol BS8 1SA, United Kingdom;* orcid.org/0000-0002-4051-6760

Dickon Young − *School of Chemistry, University of Bristol, Bristol BS8 1SA, United Kingdom*

Paul B. Krummel − *CSIRO Environment, Aspendale, VIC 3195, Australia;* orcid.org/0000-0002-4884-3678

Martin K. Vollmer − *Laboratory for Air Pollution and Environmental Technology, Empa, Swiss Federal Laboratories for Materials Science and Technology, Dübendorf 8600, Switzerland*

Stefan Reimann − *Laboratory for Air Pollution and Environmental Technology, Empa, Swiss Federal Laboratories for Materials Science and Technology, Dübendorf 8600, Switzerland*

Chris R. Lunder − *Department for Atmospheric and Climate Research, NILU-Norwegian Institute for Air Research, Kjeller 2007, Norway*

Complete contact information is available at: https://pubs.acs.org/10.1021/acs.est.4c04507

https://doi.org/10.1021/acs.est.4c04507
Environ. Sci. Technol. 2024, 58, 13318−13326

Author Contributions

Y.L., J.S., M.R., and R.G.P. are responsible for the paper design. Y.L. conducted the GEOS-Chem inversion and overall calculation. M.R. and A.G. provided the paper organization and revision. L.W. and J.M. provided the paper revision. J.K. provided the bottom-up data from Japan and WSC. S.P. and H.P. provided the measurements data at GSN station. J.M., R.F.W., P.K.S., S.O'D., D.Y., P.B.K., B.M., M.K.V., and C.R.L. provided observations from the stations. Most authors provided input to drafting the manuscript.

Notes

The authors declare no competing financial interest.

■ ACKNOWLEDGMENTS

The AGAGE inverse modeling and calibration, and the AGAGE stations at Trinidad Head, Mace Head, Ragged Point, Cape Matatula, and Kennaook/Cape Grim were supported by NASA (USA) grants 80NSSC21K1369 to MIT and 80NSSC21K1210 and 80NSSC21K1201 to SIO (and by preceding NASA grants). Mace Head is also supported by BEIS (UK) and Ragged Point by NOAA (USA) grants, both to University of Bristol. Kennaook/Cape Grim is also supported by CSIRO and the Australian Bureau of Meteorology. The AGAGE station at Gosan was supported by the Basic Science Research Program through the National Research Foundation of Korea funded by the Ministry of Education. Measurements at Jungfraujoch are supported by the Swiss National Programs HALCLIM and CLIMGAS-CH (Swiss Federal Office for the Environment [FOEN]) and by the International Foundation High Altitude Research Stations Jungfraujoch and Gornergrat (HFSJG). The AGAGE station at Zeppelin was supported by the Norwegian Environment Agency.L.M.W. received funding from the European Union's Horizon 2020 research and innovation program under Marie Skłodowska-Curie grant agreement no. 101030750. We also thank Shen Lu from Peking University and Xiao Lu from Sun Yat-Sen University for suggestions.

■ REFERENCES

(1) Burkholder, J. B.; Hodnebrog, Ø. Annex: Summary of Abundances, Lifetimes, ODPs, REs, GWPs, and GTPs; In *World Meteorological Organization (WMO). Scientific Assessment of Ozone Depletion: 2022*; 278; WMO: Geneva, 2022; p 509.

(2) Ko, M. K. W.; Newman, P. A.; Reimann, S.; Strahan, S. E. *SPARC Report No. 6: Lifetimes of Stratospheric Ozone- Depleting Substances, Their Replacements, and Related Species, in: SPARC Report WCRP-15/2013*; 2013.

(3) Totterdill, A.; Kovács, T.; Feng, W.; Dhomse, S.; Smith, C. J.; Gómez-Martín, J. C.; Chipperfield, M. P.; Forster, P. M.; Plane, J. M. C. Atmospheric Lifetimes, Infrared Absorption Spectra, Radiative Forcings and Global Warming Potentials of NF_3 and CF_3CF_2Cl (CFC-115). *Atmos. Chem. Phys.* **2016**, *16* (17), 11451−11463.

(4) Myhre, G.; Shindell, D.; Bréon, F.-M.; Collins, W.; Fuglestvedt, J.; Huang, J.; Koch, D.; Lamarque, J.-F.; Lee, D.; Mendoza, B.; Nakajima, T.; Robock, A.; Stephens, G.; Takemura, T.; Zhang, H. Anthropogenic and Natural Radiative Forcing, In: *Climate Change 2013 − The Physical Science Basis: Working Group I Contribution to the Fifth Assessment Report of the Intergovernmental Panel on Climate Change*; Cambridge University Press: Cambridge, United Kingdom and New York, NY USA, 2013; pp 659−740.

(5) Laube, C. J.; Tegtmeier, S. Substances (ODSs) and Other Gases of Interest to the Montreal Protocol, In *Scientific Assessment of Update on Ozone-DepletingOzone Depletion, GAW Report No. 278*, Chapter 1; World Meteorological Organization 2022, 2022.

(6) Arnold, T.; Harth, C. M.; Mühle, J.; Manning, A. J.; Salameh, P. K.; Kim, J.; Ivy, D. J.; Steele, L. P.; Petrenko, V. V.; Severinghaus, J. P.; Baggenstos, D.; Weiss, R. F. Nitrogen Trifluoride Global Emissions Estimated from Updated Atmospheric Measurements. *Proc. Natl. Acad. Sci. U. S. A.* **2013**, *110* (6), 2029−2034.

(7) Arnold, T.; Manning, A. J.; Kim, J.; Li, S.; Webster, H.; Thomson, D.; Mühle, J.; Weiss, R. F.; Park, S.; O'Doherty, S. Inverse Modelling of CF_4 and NF_3 Emissions in East Asia. *Atmospheric Chemistry and Physics* **2018**, *18* (18), 13305−13320.

(8) Fthenakis, V.; Clark, D. O.; Moalem, M.; Chandler, P.; Ridgeway, R. G.; Hulbert, F. E.; Cooper, D. B.; Maroulis, P. J. Life-Cycle Nitrogen Trifluoride Emissions from Photovoltaics. *Environ. Sci. Technol.* **2010**, *44* (22), 8750−8757.

(9) Beu, L.; Raoux, S.; Chang, Y. C.; Czerniak, M. R.; Illuzzi, F.; Kitagawa, T.; Ottinger, D.; Parasyuk, N. Chapter 6 Electronics Industry Emissions. In *2019 Refinement to the 2006 IPCC Guidelines for National Greenhouse Gas Inventories*; IPCC: Switzerland, 2020.

(10) NIR, Japan, *National Greenhouse Gas Inventory Report of JAPAN 2023*, Center for Global Environmental Research, Earth System Division, National Institute for Environmental Studies; Greenhouse Gas Inventory Office of Japan and Ministry of the Environment: Japan, 2023.

(11) Papadimitriou, V. C.; McGillen, M. R.; Fleming, E. L.; Jackman, C. H.; Burkholder, J. B. NF_3: UV Absorption Spectrum Temperature Dependence and the Atmospheric and Climate Forcing Implications. *Geophys. Res. Lett.* **2013**, *40* (2), 440−445.

(12) Dillon, T. J.; Vereecken, L.; Horowitz, A.; Crowley, J. N.; Lelieveld, J.; Khamaganov, V. Removal of the Potent Greenhouse Gas NF_3 by Reactions with the Atmospheric Oxidants O(1D), OH and O_3. *Phys. Chem. Chem. Phys.* **2011**, *13* (41), 18600−18608.

(13) NDC Japan. *Japan's Nationally Determined Contribution (NDC)*, 2022. https://unfccc.int/sites/default/files/NDC/2022-06/JAPAN_FIRST%20NDC%20%28UPDATED%20SUBMISSION%29.pdf.

(14) Huang, R. *The Central People's Government of the People's Republic of China*, 2020. http://www.gov.cn/zhengce/zhengceku/2021-01/06/content_5577360.htm.

(15) NDC South Korea. Submission under the Paris Agreement. *The Republic of Korea's Enhanced Update of Its First Nationally Determined Contribution*, 2021. https://unfccc.int/sites/default/files/NDC/2022-06/211223_The%20Republic%20of%20Korea%27s%20Enhanced%20Update%20of%20its%20First%20Nationally%20Determined%20Contribution_211227_editorial%20change.pdf.

(16) UNFCCC Secretariat. *Nationally Determined Contributions under the Paris Agreement. Synthesis Report by the Secretariat*. https://unfccc.int/documents/619180?gad_source=1&gclid=EAIaIQobChMI-MS2xavqhAMV5GZHAR12PgJqEAAYASACEgKH3_D_BwE.

(17) NDC United States. *The United States' Nationally Determined Contribution: Reducing Greenhouse Gases in the United States: A 2030 Emissions Target.*, 2021. https://unfccc.int/sites/default/files/NDC/2022-06/United%20States%20NDC%20April%2021%202021%20Final.pdf.

(18) NDC EU. *Submission by Spain and the European Commission on Behalf of the European Union and Its Member States*, 2023. https://unfccc.int/sites/default/files/resource/ES-2023-09-29%20EU%20Submission%20-%20Art%202.1c%202nd%20SSH%20dialogue.pdf.

(19) NDC Canada. *Canada's 2021 Nationally Determined Contribution Under the Paris Agreement*, 2022. https://unfccc.int/sites/default/files/NDC/2022-06/Canada%27s%20Enhanced%20NDC%20Submission1_FINAL%20EN.pdf

(20) NDC Australia. *Australia's Nationally Determined Contribution.*, 2022. https://unfccc.int/sites/default/files/NDC/2022-06/Australias%20NDC%20June%202022%20Update%20%283%29.pdf.

(21) Prinn, R. G.; Weiss, R. F.; Arduini, J.; Arnold, T.; DeWitt, H. L.; Fraser, P. J.; Ganesan, A. L.; Gasore, J.; Harth, C. M.; Hermansen, O.; Kim, J.; Krummel, P. B.; Li, S.; Loh, Z. M.; Lunder, C. R.; Maione,

https://doi.org/10.1021/acs.est.4c04507
Environ. Sci. Technol. 2024, 58, 13318−13326

M.; Manning, A. J.; Miller, B. R.; Mitrevski, B.; Mühle, J.; O'Doherty, S.; Park, S.; Reimann, S.; Rigby, M.; Saito, T.; Salameh, P. K.; Schmidt, R.; Simmonds, P. G.; Steele, L. P.; Vollmer, M. K.; Wang, R. H.; Yao, B.; Yokouchi, Y.; Young, D.; Zhou, L. History of Chemically and Radiatively Important Atmospheric Gases from the Advanced Global Atmospheric Gases Experiment (AGAGE). *Earth System Science Data* **2018**, *10* (2), 985−1018.

(22) statista.com. *LCD Panel Production Capacity Share from 2016 to 2025, by Country*, 2022. https://www.statista.com/statistics/1056470/lcd-panel-production-capacity-country/.

(23) Platzer, M. D.; JFS, Jr.; Sutter, K. M. *Semiconductors: U.S. Industry, Global Competition, and Federal Policy*; 2020. https://crsreports.congress.gov/product/pdf/R/R46581.

(24) Ben, D.; Choe, S.-H. *Japan Imposes Broad New Trade Restrictions on South Korea*. 2019. https://www.nytimes.com/2019/08/01/business/japan-south-korea-trade.html.

(25) Park, S.; Western, L. M.; Saito, T.; Redington, A. L.; Henne, S.; Fang, X.; Prinn, R. G.; Manning, A. J.; Montzka, S. A.; Fraser, P. J.; Ganesan, A. L.; Harth, C. M.; Kim, J.; Krummel, P. B.; Liang, Q.; Mühle, J.; O'Doherty, S.; Park, H.; Park, M.-K.; Reimann, S.; Salameh, P. K.; Weiss, R. F.; Rigby, M. A Decline in Emissions of CFC-11 and Related Chemicals from Eastern China. *Nature* **2021**, *590* (7846), 433−437.

(26) *EDGAR V7.0. EDGAR (Emissions Database for Global Atmospheric Research)* Community GHG Database (a Collaboration between the European Commission, Joint Research Centre (JRC), 2022. the International Energy Agency (IEA), and Comprising IEA-EDGAR CO2, EDGAR CH4, EDGAR N2O, EDGAR F-GASES Version 7.0. European Commission. https://edgar.jrc.ec.europa.eu/dataset_ghg70.

(27) Guo, L.; Fang, X. Mitigation of Fully Fluorinated Greenhouse Gas Emissions in China and Implications for Climate Change Mitigation. *Environ. Sci. Technol.* **2023**, *57*, 19487.

(28) m.huaon.com, 2022. *The Competition Pattern and Prospect of China's Nitrogen Trifluoride Market in 2022, and the Demand for Highly Purified Nitrogen Trifluoride Will Grow Rapidly*. https://m.huaon.com/detail/844218.html.

(29) Adams, B. M. *Gas Market Dynamics—NF_3, Helium, Neon The Good, the Bad, and the Ugly*. 2016.

(30) Sovacool, B. K.; Griffiths, S.; Kim, J.; Bazilian, M. Climate Change and Industrial F-Gases: A Critical and Systematic Review of Developments, Sociotechnical Systems and Policy Options for Reducing Synthetic Greenhouse Gas Emissions. *Renewable and Sustainable Energy Reviews* **2021**, *141*, No. 110759.

(31) Illuzzi, F.; Thewissen, H. Perfluorocompounds Emission Reduction by the Semiconductor Industry. *Journal of Integrative Environmental Sciences* **2010**, *7* (sup1), 201−210.

(32) Kastenmeier, B. E. E.; Oehrlein, G. S.; Langan, J. G.; Entley, W. R. Gas Utilization in Remote Plasma Cleaning and Stripping Applications. *J. Vac. Sci. Technol. A* **2000**, *18* (5), 2102.

(33) Beu, L. S. *Reduction of Perfluorocompound (PFC) Emissions: 2005 State-of-the- Technology Report*; 2005. International SEMATECH Manufacturing Initiative, Inc. https://www.epa.gov/sites/default/files/2016-02/documents/final_tt_report.pdf.

(34) Kim, J.; Thompson, R.; Park, H.; Bogle, S.; Mühle, J.; Park, M.-K.; Kim, Y.; Harth, C. M.; Salameh, P. K.; Schmidt, R.; Ottinger, D.; Park, S.; Weiss, R. F. Emissions of Tetrafluoromethane (CF_4) and Hexafluoroethane (C_2F_6) From East Asia: 2008 to 2019. *J. Geophys Res. Atmos* **2021**, *126* (16), No. e2021JD034888.

(35) Arnold, T.; Mühle, J.; Salameh, P. K.; Harth, C. M.; Ivy, D. J.; Weiss, R. F. Automated Measurement of Nitrogen Trifluoride in Ambient Air. *Anal. Chem.* **2012**, *84* (11), 4798−4804.

(36) O'Doherty, S.; Simmonds, P. G.; Cunnold, D. M.; Wang, H. J.; Sturrock, G. A.; Fraser, P. J.; Ryall, D.; Derwent, R. G.; Weiss, R. F.; Salameh, P.; Miller, B. R.; Prinn, R. G. In Situ Chloroform Measurements at Advanced Global Atmospheric Gases Experiment Atmospheric Research Stations from 1994 to 1998. *J. Geophys. Res.: Atmos.* **2001**, *106*, 20429−20444.

(37) GEOS-Chem 12.5.0. *Geoschem/Geos-Chem: GEOS-Chem 12.5.0*. 2019 DOI: 10.5281/zenodo.3403111.

(38) Gelaro, R.; McCarty, W.; Suárez, M. J.; Todling, R.; Molod, A.; Takacs, L.; Randles, C.; Darmenov, A.; Bosilovich, M. G.; Reichle, R.; Wargan, K.; Coy, L.; Cullather, R.; Draper, C.; Akella, S.; Buchard, V.; Conaty, A.; da Silva, A.; Gu, W.; Kim, G.-K.; Koster, R.; Lucchesi, R.; Merkova, D.; Nielsen, J. E.; Partyka, G.; Pawson, S.; Putman, W.; Rienecker, M.; Schubert, S. D.; Sienkiewicz, M.; Zhao, B. The Modern-Era Retrospective Analysis for Research and Applications, Version 2 (MERRA-2). *J. Clim.* **2017**, *30* (13), 5419−5454.

(39) m.huaon.com, 2019. *Analysis of Technology and Demand of the Distribution of NF_3 from Global and China*. https://www.huaon.com/story/491569.

(40) An, M.; Western, L. M.; Say, D.; Chen, L.; Claxton, T.; Ganesan, A. L.; Hossaini, R.; Krummel, P. B.; Manning, A. J.; Mühle, J.; O'Doherty, S.; Prinn, R. G.; Weiss, R. F.; Young, D.; Hu, J.; Yao, B.; Rigby, M. Rapid Increase in Dichloromethane Emissions from China Inferred through Atmospheric Observations. *Nat. Commun.* **2021**, *12* (1), 7279.

(41) UNFCCC *Greenhouse Gas Inventory Data*, 2023. https://di.unfccc.int/detailed_data_by_party.

(42) Rigby, M.; Mühle, J.; Miller, B. R.; Prinn, R. G.; Krummel, P. B.; Steele, L. P.; Fraser, P. J.; Salameh, P. K.; Harth, C. M.; Weiss, R. F.; Greally, B. R.; O'Doherty, S.; Simmonds, P. G.; Vollmer, M. K.; Reimann, S.; Kim, J.; Kim, K.-R.; Wang, H. J.; Olivier, J. G. J.; Dlugokencky, E. J.; Dutton, G. S.; Hall, B. D.; Elkins, J. W. History of Atmospheric SF_6 from 1973 to 2008. *Atmospheric Chemistry and Physics* **2010**, *10* (21), 10305−10320.

(43) Bartos, S.; Beu, L. S.; Burton, C. S.; Fraust, C. L.; Illuzzi, F.; Mocella, M. T.; Raoux, S. Electronics Industry Emissions. In *IPCC guidelines for National Greenhouse Gas Inventories*; Intergovernmental Panel on Climate Change (IPCC), prepared by the National Greenhouse Gas Inventories Programme, 2006.

(44) World Semiconductor Council (WSC). *Joint Statement of the 24th Meeting of the World Semiconductor Council (WSC)*, 2020. http://www.semiconductorcouncil.org/wp-content/uploads/2020/09/24th-WSC-Joint-Statement-Final.pdf.

https://doi.org/10.1021/acs.est.4c04507
Environ. Sci. Technol. 2024, 58, 13318−13326